

Supporting Information for

Dopant-Induced Modulation of Lithium-ion
Conductivity in Cubic Garnet Solid Electrolytes: A
First-principles Study

Feye-Feng Lu,^a Hong-Kang Tian^{a, b, c}*

^a Department of Chemical Engineering, National Cheng Kung University, Tainan 70101,
Taiwan.

^b Program on Smart and Sustainable Manufacturing, Academy of Innovative Semiconductor and
Sustainable Manufacturing, National Cheng Kung University, Tainan 70101, Taiwan.

^c Hierarchical Green-Energy Materials (Hi-GEM) Research Center, National Cheng Kung
University, Tainan 70101, Taiwan

Email: hktian@gs.ncku.edu.tw

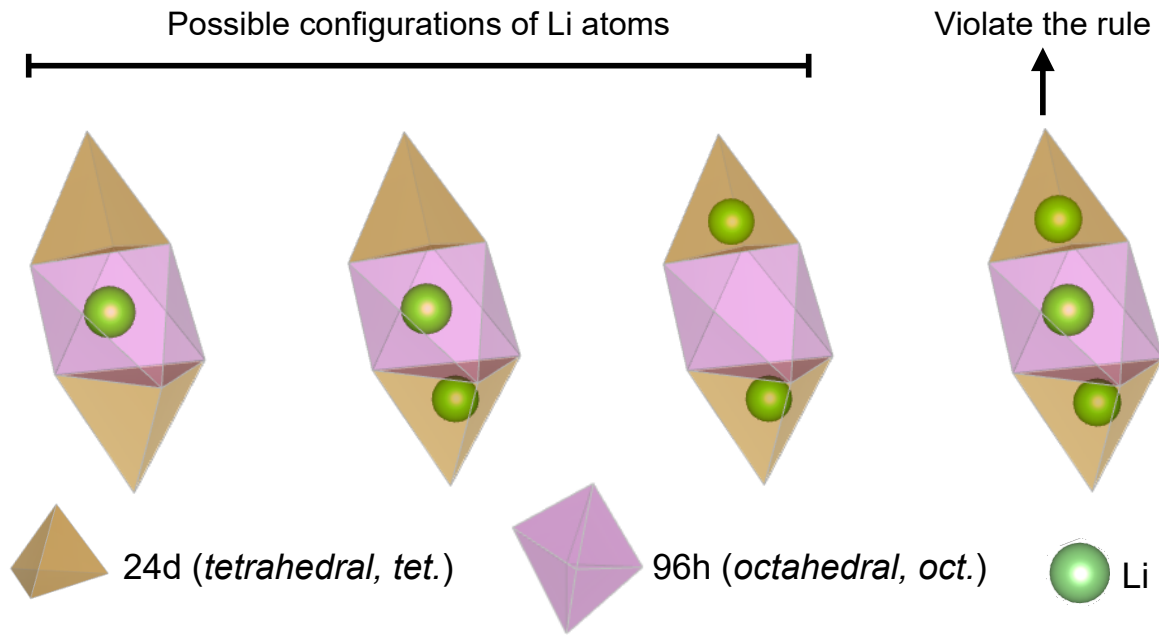


Figure S1. Possible Li distributions in c-LLZO and the scenario that violates the rule proposed by O'Callaghan et al.¹ Li atoms were randomly distributed in the first three configurations from the left in this study.

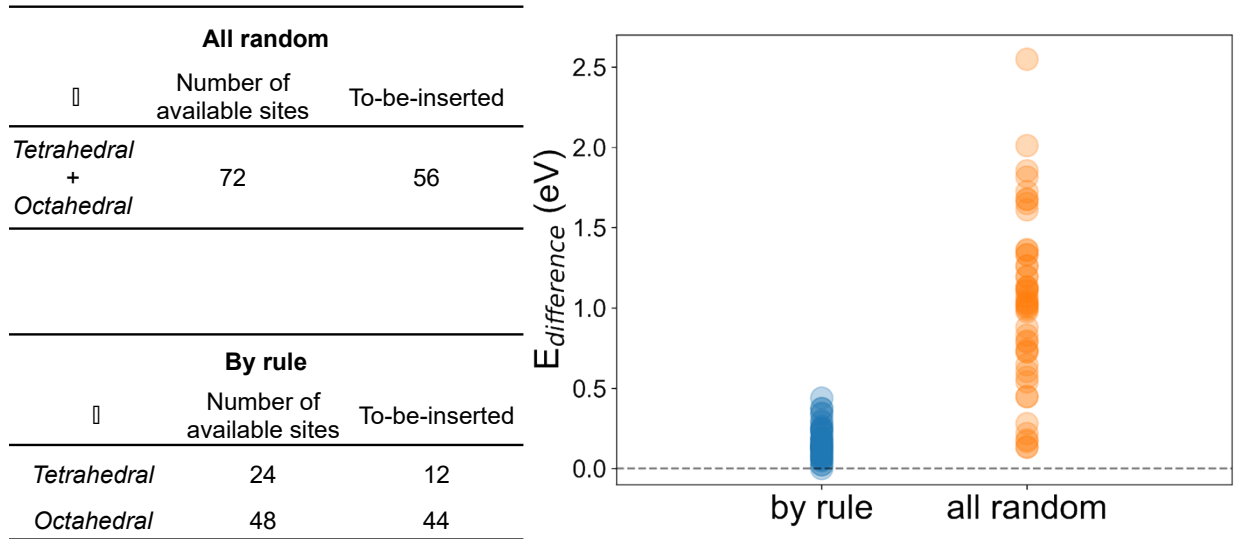


Figure S2. Comparison of two Li atom distribution scenarios in c-LLZO: all-random and by-rule. The all-random scenario depicts Li atoms randomly distributed in either *tetrahedral* or *octahedral* sites. The by-rule scenario follows the minimization principle of Li repulsion force proposed by O'Callaghan et al.,¹ with half of the *tetrahedral* sites occupied, as discussed in the main text. Li atoms are randomly distributed while maintaining a fixed number at each site and avoiding configurations that violate the minimization principle. The calculated total energies are displayed on the right, with $E_{difference}$ denoting the relative energy difference concerning the lowest energy point. A comparison of 50 distinct Li configurations for each scenario demonstrates that the by-rule principle helps maintain total energy variation within a lower range of 0.5 eV, whereas without the rule, energy fluctuations can reach up to 2.5 eV. The configuration with the lowest energy was selected for further analysis.

Table S1. Comparison between the calculated lattice parameters in this study and the experimental results.

	Calculated average lattice parameter (Å), this work	Experimental results (Å)	Deviation (%)
pure-LLZO	13.0175	13.0035 ²	0.107
Ga-doped LLZO	13.0196	12.9790 ³	0.313
Al-doped LLAO	13.0109	12.9720 ⁴	0.300
Fe-doped LLZO	13.0153	12.9800 ⁵	0.272

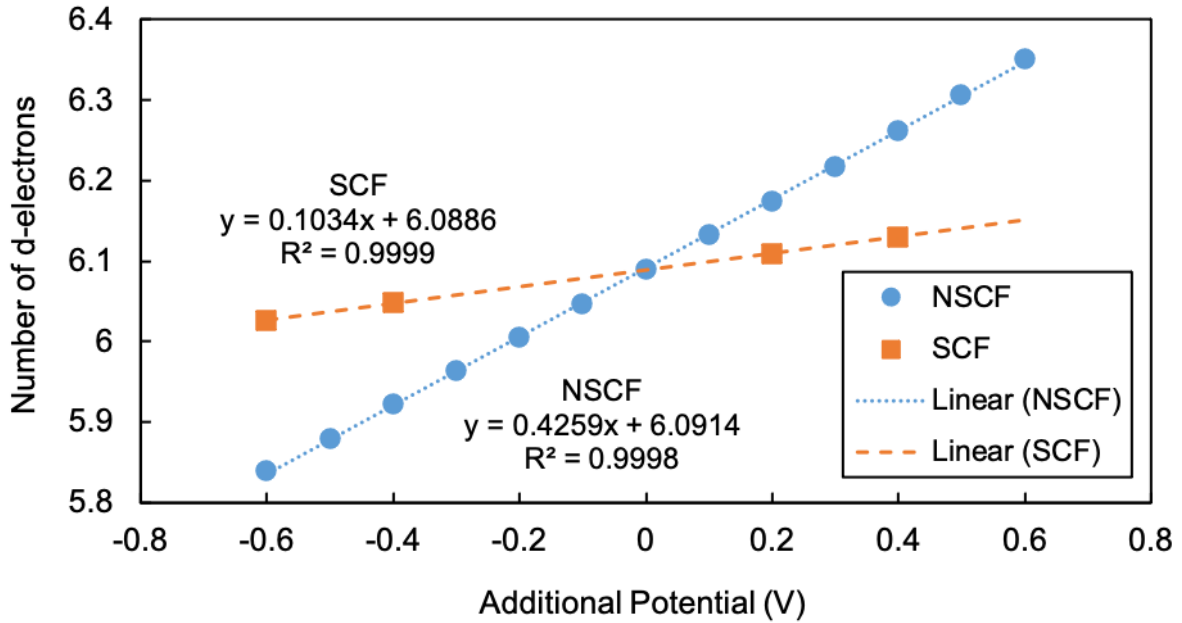


Figure S3. The number of d-electrons on the Fe atom in Fe-doped LLZO varies with a minor adjustment in the additional potential applied to the Fe atom. This linear response method was proposed by Cococcioni et al.⁶ NSCF refers to non-self-consistent field calculations, while SCF denotes self-consistent field calculations. Due to convergence issues, some SCF calculations at certain potentials did not converge. Consequently, only the converged data are presented here. Nonetheless, despite the convergence issues, the SCF data points still exhibit a clear linear trend. The suitable Hubbard U values for GGA+ U calculations of Fe-LLZO can be determined by the slopes of the two linear lines fitted to the data, as:

$$U = \frac{1}{0.1034} - \frac{1}{0.4259} = 7.32 \text{ eV}$$

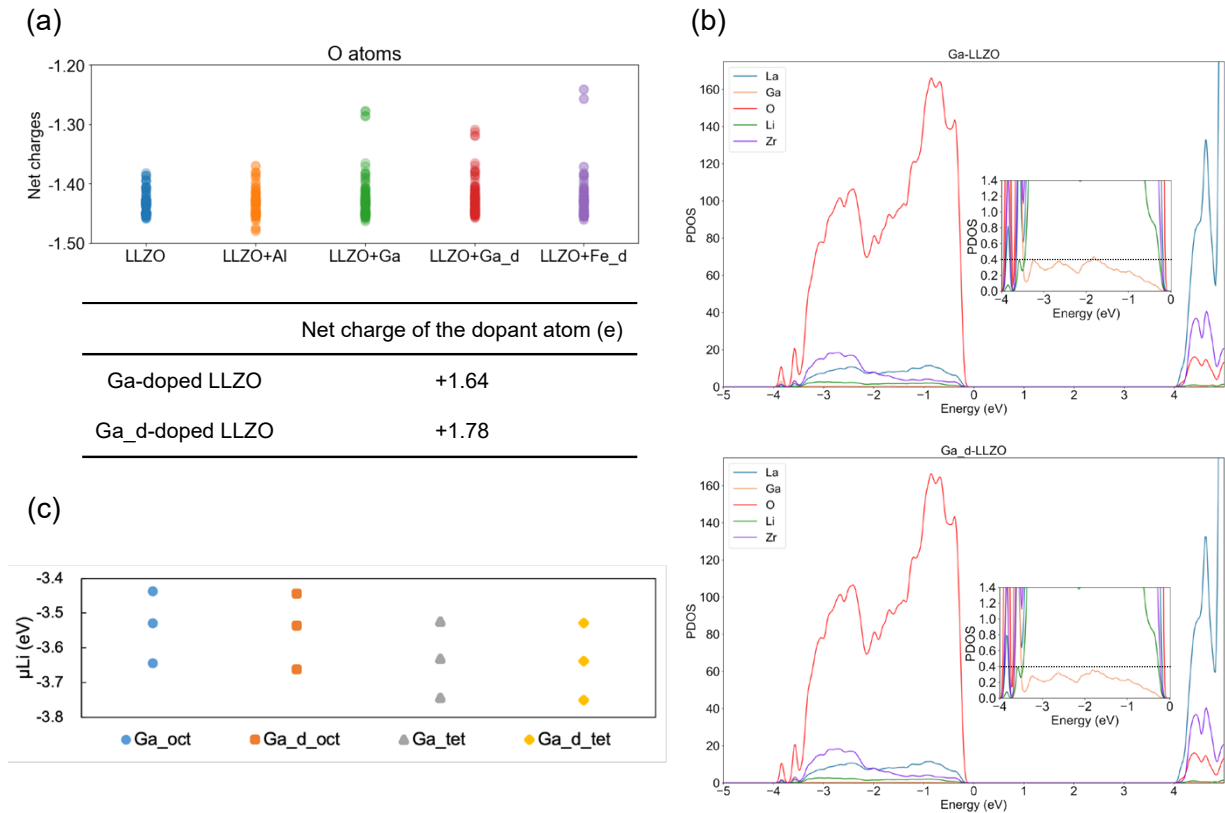


Figure S4. The comparison of using Ga ($4s^24p^1$) and Ga_d ($3d^{10}4s^24p^1$) as Projector Augmented Wave (PAW) potentials in Ga-doped LLZO. (a) shows net charge results for Oxygen atoms and Ga atom are depicted using Bader charge analysis. The Ga_d atom exhibits a slightly positive net charge, consistent with the slightly reduced O atom charges. (b) illustrates the Partial Density of States (PDOS), which displays nearly identical curves and energy levels. The only distinction arises in the intensity of the Ga state near the Fermi level (Energy = 0 eV), where Ga_d exhibits a lower intensity that corresponds to the net charge value. (c) displays the calculated Li chemical potential, with slightly smaller values observed for Ga_d compared to Ga. However, overall, the values are very similar between the two, indicating a close resemblance in their impact on the system.

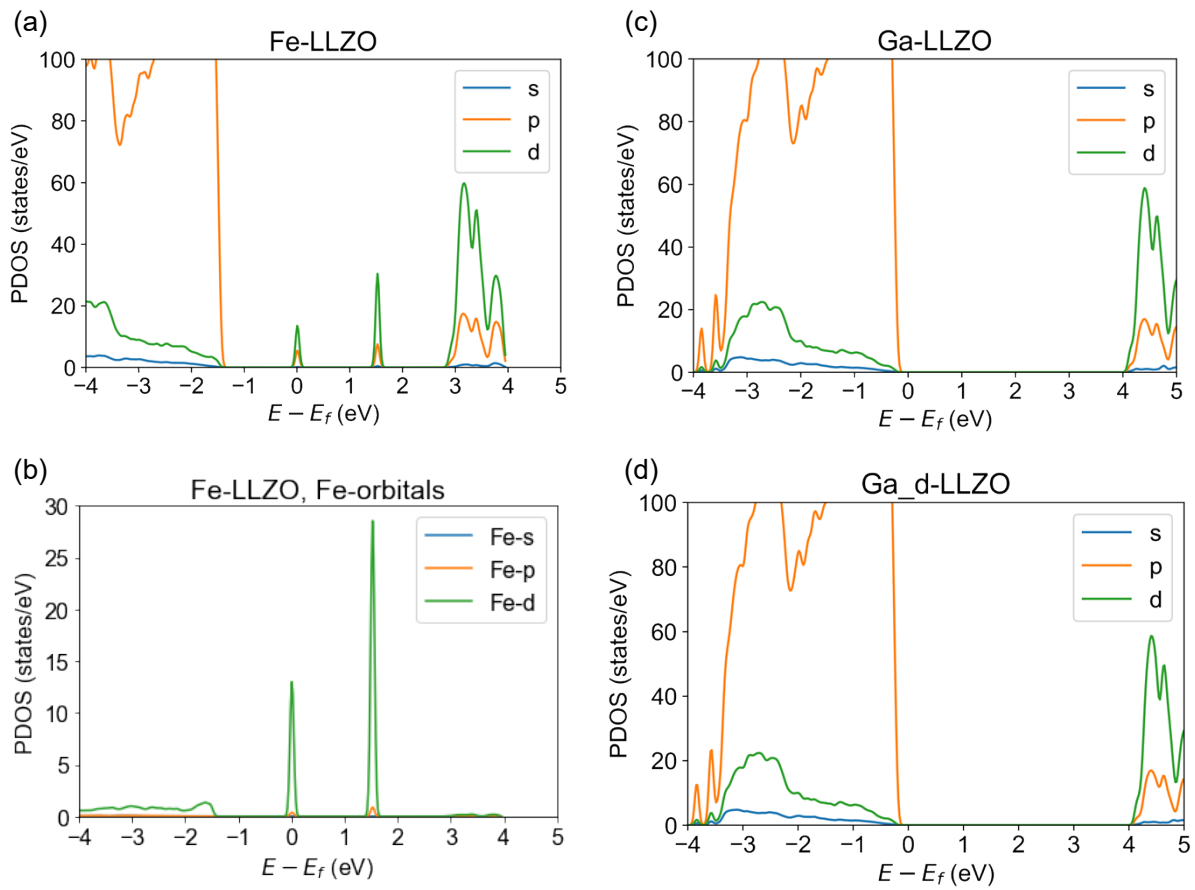


Figure S5. The orbital PDOS for different systems. (a) is the orbital PDOS for Fe-LLZO and Ga-LLZO, while (c) and (d) depict the orbital PDOS for Ga-LLZO using Ga PAW potential and Ga_d PAW potential, respectively. Additionally, (b) represents the orbital PDOS solely for the Fe atom in Fe-LLZO.

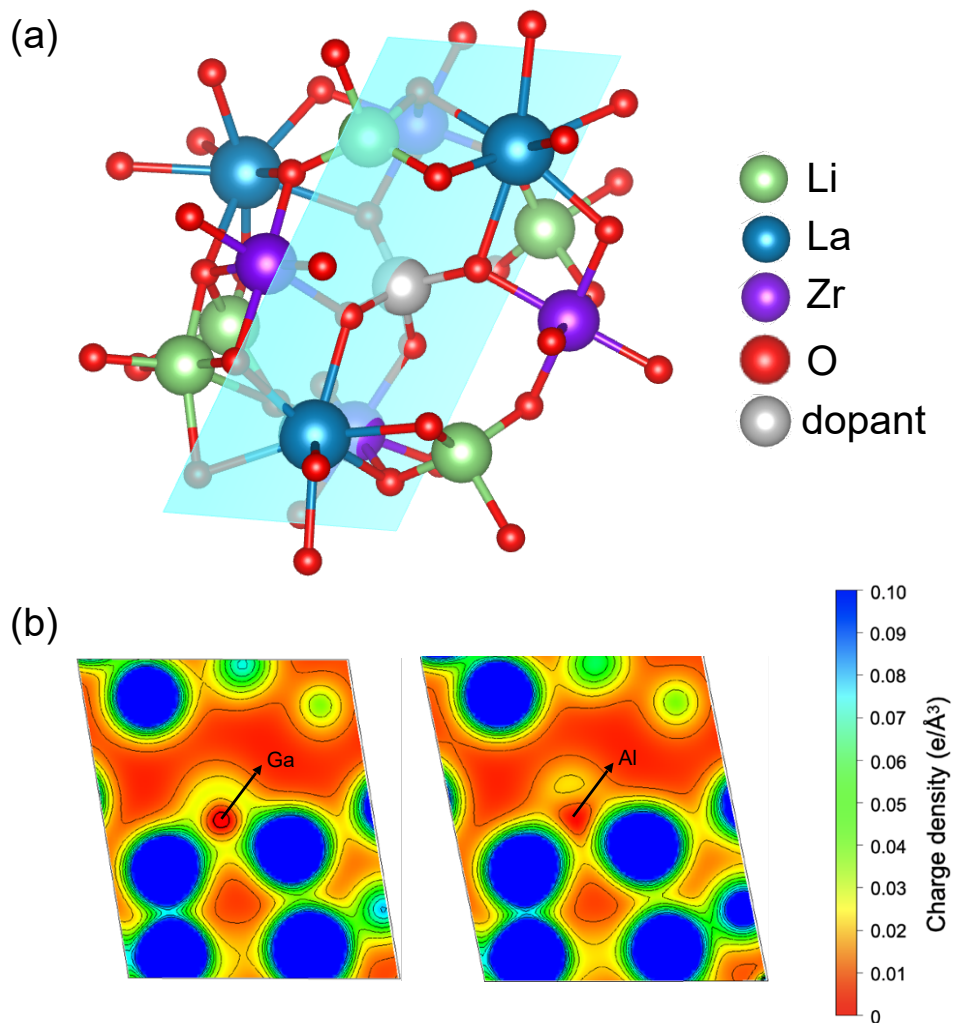


Figure S6. (a) Illustration of the sliced plane in doped-LLZO structures for charge density plotting. (b) Calculated charge density on the corresponding 2D plane for Ga-doped and Al-doped LLZO. The presence of more yellow regions surrounding the Ga dopant atom compared to the Al dopant atom indicates a higher retention of electrons with Ga. This observation aligns with the findings from the Projected Density of States (PDOS) and Bader charge analysis in the main text.

References

- (1) O'Callaghan, M. P.; Cussen, E. J. Lithium Dimer Formation in the Li-Conducting Garnets $\text{Li}_{5+x}\text{BaxLa}_3\text{-XTa}_2\text{O}_{12}$ ($0 < x \leq 1.6$). *Chemical Communications* **2007**, No. 20, 2048–2050.
- (2) Xie, H.; Alonso, J. A.; Li, Y.; Fernández-Díaz, M. T.; Goodenough, J. B. Lithium Distribution in Aluminum-Free Cubic $\text{Li}_7\text{La}_3\text{Zr}_2\text{O}_{12}$. *Chemistry of Materials* **2011**, 23 (16), 3587–3589.
- (3) Wagner, R.; Redhammer, nther J.; Rettenwander, D.; Senyshyn, A.; Schmidt, W.; Wilkening, M.; Amthauer, G.; Maier-Leibnitz Zentrum, H. Crystal Structure of Garnet-Related Li-Ion Conductor $\text{Li}_{7-3x}\text{Ga}_x\text{La}_3\text{Zr}_2\text{O}_{12}$: Fast Li-Ion Conduction Caused by a Different Cubic Modification? **2016**.
- (4) Djenadic, R.; Botros, M.; Benel, C.; Clemens, O.; Indris, S.; Choudhary, A.; Bergfeldt, T.; Hahn, H. Nebulized Spray Pyrolysis of Al-Doped $\text{Li}_7\text{La}_3\text{Zr}_2\text{O}_{12}$ Solid Electrolyte for Battery Applications. *Solid State Ion* **2014**, 263, 49–56.
- (5) Wagner, R.; Redhammer, G. J.; Rettenwander, D.; Tippelt, G.; Welzl, A.; Taibl, S.; Fleig, J.; Franz, A.; Lottermoser, W.; Amthauer, G. Fast Li-Ion-Conducting Garnet-Related $\text{Li}_{7-3x}\text{Fe}_x\text{La}_3\text{Zr}_2\text{O}_{12}$ with Uncommon $I\bar{4}3d$ Structure. *Chemistry of Materials* **2016**, 28 (16), 5943–5951.
- (6) Cococcioni, M.; De Gironcoli, S. Linear Response Approach to the Calculation of the Effective Interaction Parameters in the LDA+U Method. *Phys Rev B Condens Matter Mater Phys* **2005**, 71 (3).